[24]R. Stedman, L. Almqvist, and G. Nilsson, Phys. Rev. 162, 549 (1967).
[25]G. Gilat and L. J. Raubenheimer, Phys. Rev. 144, 390 (1966).
[26]V. V. Goldman, G. K. Horton, and M. L. Klein, Phys. Rev. B 4, 567 (1971).
[27]R. Balzer, D. S. Kupperman, and R. O. Simmons, Phys. Rev. B 4, 3636 (1971).
[28]N. S. Gillis, N. R. Werthamer, and T. R. Koehler, Phys. Rev. 165, 951 (1968).
[29]V. V. Goldman, G. K. Horton, and M. L. Klein, J. Low Temp. Phys. 1, 391 (1969).
[30]V. V. Goldman, Phys. Rev. 174, 1041 (1968).
[31]W. C. Sauder, J. Appl. Phys. 37, 1495 (1966).
[32]J. Schelten and F. Hossfeld, J. Appl. Cryst. 4, 210 (1971).
[33]W. Marshall and R. Stuart, in *Inelastic Scattering of Neutrons in Solids and Liquids* (International Atomic Energy Agency, Vienna, 1961), p. 75.
[34]V. Ambegaokar, J. M. Conway, and G. Baym, in *Lattice Dynamics*, edited by R. F. Wallis (Pergamon, New York, 1965), p. 261.
[35]T. H. K. Barron and M. L. Klein, Proc. Phys. Soc. (London) 85, 533 (1965).
[36]J. A. Barker, M. L. Klein, and M. V. Bobetic, Phys. Rev. B 2, 4176 (1970).

PHYSICAL REVIEW B VOLUME 6, NUMBER 12 15 DECEMBER 1972

Strain Dependence of Longitudinal Piezoelectric, Elastic, and Dielectric Constants of *X*-Cut Quartz*

R. A. Graham
Sandia Laboratories, Albuquerque, New Mexico 87115
(Received 10 July 1972)

Experimental measurements of the piezoelectric current from impact-loaded *X*-cut quartz are utilized to determine the finite-strain piezoelectric and elastic constitutive relations for uniaxial strain η_1 from 2.4×10^{-3} to 4.3×10^{-2}. The measurements are analyzed to provide values for the linear piezoelectric stress constant e_{11}, the direct-effect nonlinear constant $\partial e_{11}/\partial\eta_1$, the strain dependence of the permittivity, and the second-, third-, and fourth-order longitudinal elastic constants. It is found that consitutive relations developed to describe nonlinear responses at small strains describe the response of *X*-cut quartz for the large strains employed in the present investigation. The results show that $e_{11}=(0.1711\pm0.000\,94)$ C m^{-2}, $\partial e_{11}/\partial\eta_1=-2.64\pm0.048$ C m^{-2}, and $\epsilon_{11}^{-1}\partial\epsilon_{11}/\partial\eta_1=-0.46\pm0.13$. The elastic constants are $c_{11}=(0.868\pm0.0095)\times10^{12}$ dyn cm^{-2}, $c_{111}=(-3.0\pm0.3)\times10^{12}$ dyn cm^{-2}, and $c_{1111}=+(75\pm25)\times10^{12}$ dyn cm^{-2}. Data from previous authors are analyzed to obtain values for the nonlinear piezoelectric constants at 573 and 79 °K.

I. INTRODUCTION

This paper reports measurements of nonlinear elastic and piezoelectric constitutive relations for *X*-cut α quartz.[1] Elastic shock-compression responses are utilized to measure the piezoelectric stress constant e_{11}, the strain dependence of e_{11}, the strain dependence of the permittivity, and the strain dependence of the longitudinal elastic constants. The measurements are accomplished for elastic compressions of from 2.4×10^{-3} to 4.3×10^{-2}. The present work is the first quantitative experimental determination of a nonlinear piezoelectric constitutive relation.

An elastic shock wave is introduced into each sample by subjecting the *X*-cut quartz disk to a precisely controlled planar impact. As a result of the impact, a shock wave traverses the disk causing a current to flow in a low-impedance resistive circuit connecting electrodes on the faces of the disk. The current pulse is a result of the direct piezoelectric effect[2]; as such, the current provides a direct measure of the piezoelectric polarization of the shock-loaded sample. Since *X*-cut quartz remains elastic to strains of 4.3×10^{-2}, the contributions of the nonlinear piezoelectric and elastic constants are large and may be readily detected.

Various nonlinear acoustic effects in elastic solids were recently reviewed by Zarembo and Krasil'nikov.[3] Of particular interest are the nonlinear interactions of acoustic and microwave electric fields in piezoelectric solids which lead to unique electrical responses at microwave frequencies.[4] Although the microwave experiments have demonstrated the existence of the nonlinear interactions, the nonlinear piezoelectric constants have not yet been measured. Acoustic second-harmonic-generation experiments in *X*-cut quartz have shown the existence of nonlinear piezoelectric responses; however, the experiments provided only an order-of-magnitude estimate for the nonlinear piezoelectric constant.[5,6]

Third-order elastic constants characteristic of the unstrained state have been determined for a number of solids.[3,7] The present investigation ex-

tends these measurements by several orders of magnitude in strain amplitude. Recently, third- and fourth-order longitudinal elastic constants were determined for sapphire and fused quartz in a manner similar to that employed in the present investigation.[8]

Previous investigations of short-circuited piezoelectric currents from shock-loaded X-cut quartz have served to delineate the principal features of the piezoelectric response for stresses from 2.6 to 300 kbar.[9–13] In this stress range, drastically different current-vs-time pulses are observed which range from those which can be described in terms of linear elastic constitutive relations to those which must be described with highly nonlinear inelastic and electrical properties. The principal observations of these earlier investigations were that X-cut quartz exhibits (i) a very large elastic limit under shock loading,[10,14,15] (ii) a small increase in piezoelectric constant with compression,[11] and (iii) distortion of current-time waveforms due to shock-induced conductivity in the elastic range.[12,13]

This paper is organized in the following way. Nonlinear constitutive relations for elastic and piezoelectric solids are presented in Sec. II. The experimental arrangement is then described in Sec. III. An electrostatic model is developed in Sec. IV to relate the measured displacement currents to the strain-induced piezoelectric polarization. Following the presentation of results in Sec. V, the various piezoelectric elastic constants and dielectric constants are compared to related work in Sec. VI. Data from previous authors are analyzed to obtain the temperature dependence of the nonlinear piezoelectric constant. Finally the principal results of the investigation are summarized in Sec. VII.

II. NONLINEAR CONSTITUTIVE RELATIONS

Nonlinear constitutive equations describing the elastic response of materials are frequently developed from expansions of strain energy in powers of a finite-strain measure. When truncated after the first or second nonlinear term, the equations have been successfully used to describe nonlinear effects observed at small strains.[16] The applicability of these equations to the description of solids at the large elastic compressions employed in the present investigation remains to be demonstrated. In this regard, the quantitative values obtained for the nonlinear coefficients in the present experiments provide an explicit measure of the applicability of the expansions to the large strains employed.

While general concepts in nonlinear elasticity are well established, the extension of the theory to include electrical effects is nontrivial and is the subject of active investigation by Toupin,[17] Eringen,[18] and Tiersten.[19] Toupin[17] first pointed out that considerations of invariance indicate that the use of local polarization, not the macroscopic electric field, leads to rotationally invariant equations. Since the present investigation is restricted to one-dimensional measurements, rotational invariance need not be invoked, and the interpretation of the measurements will be based on constitutive equations which employ the electric field.[20] It should be noted that the experimental data themselves will be used to justify the form of the piezoelectric constitutive relation.

A. Nonpiezoelectric Elastic Solids

Following Thurston,[16] finite deformations are described in terms of a coordinate system (a_1, a_2, a_3) which identifies a material particle and a coordinate system (x_1, x_2, x_3) which identifies a spatial position. The x_i are spatial or Eulerian coordinates and the a_i are material or Lagrangian coordinates. The displacement d_i may be written

$$d_i = x_i - a_i\,, \quad i = 1, 2, 3\,. \tag{1}$$

Lagrangian or material strains η_{jk} are then defined as the difference of the squares of the lengths of line elements as

$$2\eta_{jk}da_j da_k = dx_i\,dx_i - da_i\,da_i\,, \tag{2}$$

where the Einstein summation is used. The constitutive relation will be developed from an expansion of internal energy $\overline{U}$ at constant entropy s. It is convenient to define a thermodynamic tension

$$t_{km} = \rho_0 \left(\frac{\partial \overline{U}}{\partial \eta_{km}}\right)_s$$

and elastic constants of the form

$$c^s_{ijkl} = \left(\frac{\partial t_{ij}}{\partial \eta_{kl}}\right)_s\,. \tag{3}$$

Expanding the internal energy $\overline{U}(\eta, s)$ about the unstrained state, we find

$$[\overline{U}(\eta, s) - \overline{U}(0, s)] = \tfrac{1}{2} c^s_{ijkl}\eta_{ij}\eta_{kl} + \tfrac{1}{6} c^s_{ijklmn}\eta_{ij}\eta_{kl}\eta_{mn} + \tfrac{1}{24} c^s_{ijklmnpq}\eta_{ij}\eta_{kl}\eta_{mn}\eta_{pq} + \cdots\,. \tag{4}$$

Hence,

$$t_{ij} = c^s_{ijkl} + \tfrac{1}{2} c^s_{ijklmn}\eta_{ij}\eta_{kl} + \tfrac{1}{6} c^s_{ijklmnop}\eta_{ij}\eta_{kl}\eta_{mn} + \cdots + \text{higher-order terms (h. o. t.)}\,. \tag{5}$$

Since the present experiments are concerned only with longitudinal response in uniaxial strain, Eq. (5) is specialized with more compact notation to yield

$$t_1 = c^s_{11}\eta_1 + \tfrac{1}{2} c^s_{111}\eta_1^2 + \tfrac{1}{6} c^s_{1111}\eta_1^3 + \cdots + \text{h. o. t.}\,, \tag{6}$$

where c_{11}^s, c_{111}^s, and c_{1111}^s represent isentropic second-, third-, and fourth-order elastic constants. Unlike conventional experiments which evaluate high-order elastic constants at low strain, the present paper will interpret the coefficients of Eq. (6) as those which define the expansion over the range of elastic compressions achieved in the experiments.

B. Piezoelectric Elastic Solids

The piezoelectric constitutive relation is formulated as for the elastic solid except that the internal energy is further considered to be a function of the electric field E. The internal energy function $\overline{U} = \overline{U}(\eta, s, E)$ is expanded at constant entropy. When the derivatives of this expansion, $t = \rho_0(\partial \overline{U}/\partial \eta)$ and $D = \rho_0(\partial \overline{U}/\partial E)$, are specialized to uniaxial strain and electric field, the constitutive relations are

$$t_1 = c_{11}^E \eta_1 + \tfrac{1}{2} c_{111}^E \eta_1^2 - e_{11} E_1 - \tfrac{1}{2} \frac{\partial e_{11}}{\partial E_1} E_1^2 - \frac{\partial e_{11}}{\partial \eta_1} \eta_1 E_1 + \tfrac{1}{6} c_{1111}^E \eta_1^3 + \text{h. o. t.} \quad (7)$$

and

$$D_1 = e_{11}\eta_1 + \tfrac{1}{2} \frac{\partial e_{11}}{\partial \eta_1} \eta_1^2 + \epsilon_1 E_1 + \tfrac{1}{2} \frac{\partial \epsilon_1}{\partial E_1} E_1^2 + \frac{\partial \epsilon_{11}}{\partial \eta_1} \eta_1 E_1 + \text{h. o. t.}\ , \quad (8)$$

where ϵ_{11} is the permittivity at constant strain.

The present experiments are conducted with the electrodes connected with an effective electrical short circuit. This condition imposes time-variable electric fields in the sample and greatly complicates exact analysis of the data. Fortunately, however, the interaction among the elastic and piezoelectric constants in X-cut quartz is smaller than the experimental errors, and the interactions can be neglected in the evaluation of Eq. (7). Hence, in determining the elastic constitutive constants for X-cut quartz the "weak-coupling" approximation will be employed. This has the effect of interpreting the data as if the piezoelectric contribution to stiffness were zero even though the experiment involves a small contribution to each constant from the piezoelectric stiffening. This contribution is equal to 0.86% of c_{11}^E in the linear theory.[21] Thurston *et al.*[22] have noted that differences between third-order constants in quartz due to different electrical boundary conditions were too small to be detected. Thus, the weak-coupling approximation should provide an excellent approximation to the experiment. To emphasize the approximation, however, the notation specifying the electrical boundary condition is dropped from the elastic constitutive relation.

All the terms in the piezoelectric constitutive relation, Eq. (8), are of potential influence. Carr[5] has estimated a value of $\partial \epsilon_1/\partial E_1 = -10^{-22}$ C V^{-2} which will have a negligible contribution of less than 0.1% in ϵ_{11} at the maximum field encountered in the present experiments. Equations (7) and (8) are then reduced to

$$t_1 = c_{11}\eta_1 + \tfrac{1}{2} c_{111}\eta_1^2 + \tfrac{1}{6} c_{1111}\eta_1^3 + \text{h. o. t} \quad (9)$$

and

$$D_1 = \left(e_{11} + \frac{1}{2} \frac{\partial e_{11}}{\partial \eta_1} \eta_1\right)\eta_1 + \left(\epsilon_{11} + \frac{\partial \epsilon_{11}}{\partial \eta_1} \eta_1\right) E_1 + \text{h. o. t}\ . \quad (10)$$

The experimental results will be expressed in terms of the nonlinear elastic and piezoelectric constitutive relations given in Eqs. (9) and (10). The analysis will be accomplished in such a way as to determine the applicability of the form of the constitutive relations to the observed large-strain behavior of quartz and to determine the appropriate constants.

Before proceeding with the development of an electrostatic model which relates the experimental observations to the constitutive relations, it will be helpful to describe the experimental configuration.

III. EXPERIMENTAL

The experimental data are obtained from samples in a one-dimensional configuration in which planar elastic shock waves are introduced by precisely controlled planar impacts. As the elastic shock wave imparted by the impact propagates through the sample, the resulting short-circuited current pulse is recorded. These current-vs-time pulses may then be analyzed with an electrostatic model to obtain values for the piezoelectric polarization, the wave speed, and the ratio of strained to unstrained permittivity at each of a number of different strain amplitudes. The strain amplitudes are chosen to have values which range from those in which nonlinear contributions are negligible to those in which nonlinear contributions are substantial.

The planar-impact technique is now widely and routinely employed to measure both electrical[23] and mechanical[24] responses of shock-loaded solids. Considerable improvement in the critical details of the experimental technique have been accomplished since the previous study[11] of the response of shock-loaded quartz. Experimental details were recently described[25]; hence, only the main features of the technique will be described here.

As shown in Fig. 1, X-cut quartz specimen disks are encapsulated in Epoxy potting and attached to the muzzle of a compressed-gas gun.[26] The projectile, faced with an X-cut quartz disk, is accelerated down the evacuated barrel and impacted upon the specimen with precise control on the alignment of the impacting surfaces. Immediately prior

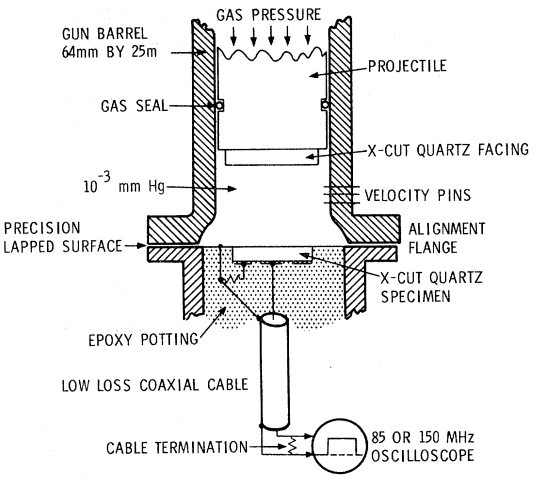

FIG. 1. Elastic shock waves are introduced into X-cut quartz samples by the precisely controlled impact of projectiles faced with X-cut quartz disks. As the elastic shock wave propagates through the sample, the resulting short-circuited piezoelectric current is monitored with a low-impedance resistive circuit connecting the two electrodes. Immediately prior to impact, the velocity of the projectile is measured to an absolute accuracy of $\pm 0.1\%$. Impact velocities of from 27 to 510 m sec^{-1}, corresponding to strains of from 2.4×10^{-3} to 4.3×10^{-2}, were utilized in the present investigation. The sample is constructed with a peripheral guard ring which ensures states of uniaxial strain, uniaxial piezoelectric polarization, and uniaxial electric field along the x axis of the quartz disk.

to impact, the velocity of the projectile is measured by coaxial pins which protrude through the side of the barrel. The short-circuited current from the specimen is monitored with a low-impedance resistive circuit, displayed on a high-frequency oscilloscope, and recorded on high-speed Polaroid film. Thus, the apparatus produces a well-controlled impact between identical materials and provides an accurate measure of the projectile velocity as well as an accurate measure of the current-time pulse from the shock-loaded sample. Various strain values are achieved by experiments at various preselected velocities; the present experiments were conducted from 27 to 510 m sec^{-1}.

Due to the symmetry of the impact of identical materials, the particle velocity u imparted to the specimen is

$$u = \tfrac{1}{2}u_0 ,$$

where u_0 is the velocity of the projectile at impact. The projectile velocity is measured with a maximum error of 0.1%.

The diameters and thicknesses of the specimen and projectile facing disks are chosen to prevent unloading from lateral surfaces during a single wave transit time. This ensures a state of uniaxial strain in the specimen. The thickness of the facing disk is chosen to control the arrival time of the unloading from the rear of the facing. In most cases the unloading time was longer than the shock-wave transit time through the sample. Some of the data were obtained during the previously reported study of the unloading response of X-cut quartz.[13] In those cases the thickness of the facing disk was chosen to cause unloading at preselected times.

The specimen is constructed from a large diameter to thickness disk with a peripheral guard ring applied to the electrode opposite the impact face. It has previously been demonstrated that a configuration in which the width of the guard ring is equal to or greater than 1.5 times the thickness of the disk will ensure states of one-dimensional strain and electric field in the central region of the disk for one wave transit time.[11] The present experiments confirm that observation. However, at the very low impact velocities, i.e., <80 m sec^{-1}, it was noted that wider guard-ring widths were required to obtain current pulses which agreed with the electrostatic model. This latter condition is apparently due to impacts occurring first at the peripheral area of the disk; the resulting signal from the guard-ringed area is then coupled electrostatically into the inner electrode signal.

The piezoelectric effect produces very large electric fields; (10^4–10^6 V cm^{-1}); hence, considerable care is taken to ensure excellent electrical insulation on the lateral edges of the disk and in the insulating gap cut between the inner electrode and the guard ring. The insulating gap has an area typically 3% of the area of the inner electrode. The effective collecting area of the inner electrode is taken to include one-half the area of the insulating gap.

Each specimen is visually inspected for defects under a strong side light. The material investigated was synthetic quartz grown by Sawyer Research Products and cut to the disk configuration by the Valpey–Fisher Corp. Each experiment is destructive; hence, variation in material properties from sample to sample will introduce statistical errors. Statistical errors due to sample-to-sample variation of properties were observed to be less than the experimental errors.

Planar impact is assured by rigidly controlling all dimensions contributing to the alignment. For the thick impactors used in the present investigation the median deviation from a planar impact, called "tilt," was 250 μrad. Experiments for impact velocities less than 50 m sec^{-1} require exceptional control on alignment. A median value of tilt of 150 μrad was achieved.

The velocity imparted to each specimen is known to a maximum error of 0.1%; hence, the accuracy of the piezoelectric constants is limited by the ab-

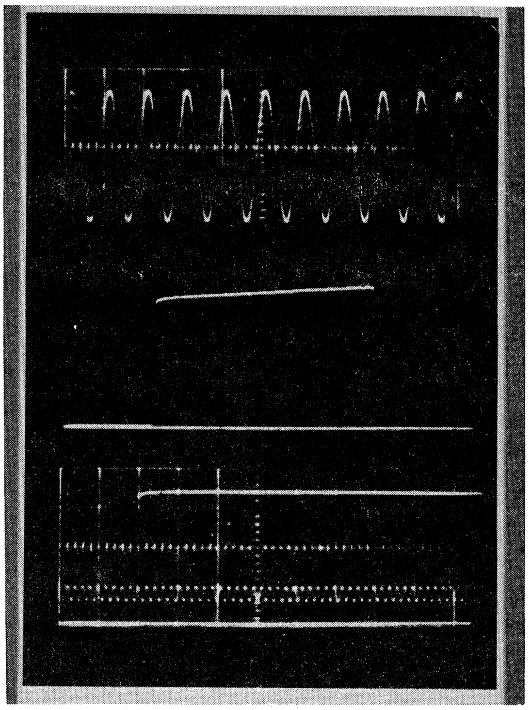

FIG. 2. Current amplitude vs time for a typical oscilloscope record is shown in the center trace. Time increases from left to right. The upper and lower traces are amplitude and timing calibration records taken immediately following the experiment. About 450 nsec prior to impact, the trace is triggered. The impact is indicated by the sharp jump in current followed by a gradual increase in current to shock-wave transit time which is indicated by a sharp decrease in signal amplitude 1.11 μsec after impact. The current amplitude is 0.67 A at a strain of 2.8×10^{-2}.

solute accuracy of the current–vs–time-pulse measurements. The considerable care and special calibrations employed to give an over-all maximum experimental error of between $\frac{1}{2}$ and 1% have been previously described in the technique article.[25]

A typical current-vs-time record is shown in Fig. 2. The response shows a jump to a first steady current value followed by a slight linear increase in current up to wave transit time. Note that the transit time of the shock wave through the sample is marked by a sharp discontinuity in current. Features of this current pulse will be interpreted in terms of the electrostatic model developed in Sec. IV.

IV. PIEZOELECTRIC-PULSE ANALYSIS

The experiments provide measures of the particle velocities imparted to the samples, the transit time of the elastic shock waves through known thicknesses, and the time-resolved amplitude of the short-circuited current. In this section the relationships among these experimental measurements and the corresponding elastic, piezoelectric, and dielectric properties will be established. The conservation of mass and momentum are used to compute the stress and linear strain, while an electrostatic analysis is used to determine piezoelectric polarization from the current-pulse measurement. Finally, a small correction is applied to the electrostatic analysis to include the effect of electromechanical coupling.

A. Characterization of Elastic Shock Waves

Shock waves in solids have been extensively utilized to determine the very high-pressure equation of state.[27] At very high pressure the solid is typically considered to react as a fluid since the pressure greatly exceeds the shear strength of the solid.[28] At lower pressures the solid may be treated as an elastic-plastic solid.[29] In the present case the solid has an unusually large shear strength, and stress amplitudes are limited to values less than that required to exceed the shear strength. In spite of the different material properties, the characterization of the shock compression may be accomplished with the conservation of momentum and mass across the shock front.

Consider a steady nondissipative elastic shock wave moving into an unstressed medium at rest. Behind the shock front the material moves with a particle velocity u and is stressed to a longitudinal stress σ. The conservation of momentum across the shock front may be expressed as

$$\sigma_1=\rho_0 U u\,, \tag{11}$$

where σ_1 is the component of compressive stress in the propagation direction, ρ_0 the unstressed density, u the particle velocity imparted by the shock front, and U the shock-wave velocity. [In the low-strain limit, $U=(c_{11}/\rho_0)^{1/2}$.] From the conservation of mass across the shock front, the uniaxial compression γ can be written as

$$\gamma=u/U\,. \tag{12}$$

The experiments provide a measure of both U and u; therefore, sufficient data are obtained to compute both the linear uniaxial compression and the stress achieved in each experiment.

The material-strain measure which includes quadratic differential elements, Eq. (2), can be computed from each linear compression point through the coordinate transformation which was formally developed by Fowles.[15] Thus, in uniaxial compression,

$$\eta_1=\gamma(\tfrac{1}{2}\gamma-1)\,. \tag{13}$$

Similarly, the thermodynamic tension, which is used to compute the high-order constants, Eq. (3), can be computed from the stress by the transformation

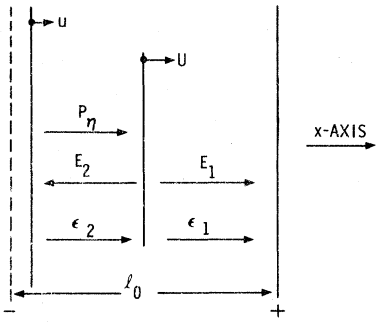

FIG. 3. Electrostatic model used to interpret the current-vs-time records is depicted by a section through the uniaxial sample at a typical time. The shock front, moving from left to right at a velocity U, divides the sample into two characteristic regions. Behind the front, the sample is strained to a constant value of piezoelectric polarization P_η. To accommodate the electric short circuit between the two electrodes, electric fields E_1 and E_2 are developed in both the strained and unstrained regions. The strained permittivity ϵ_2 and unstrained permittivity ϵ_1 are characteristic of the two regions. The left electrode moves with a velocity u which acts to cause a small decrease in thickness in time.

$$t_1 = \sigma_1(\gamma - 1)^{-1} . \tag{14}$$

The shock-induced temperature rise due to adiabatic compression can be readily computed. At the maximum compression utilized in these experiments, the temperature rise is 10 °C. This increase in temperature will cause fractional changes in the elastic stiffness c_{11}, the piezoelectric stress constant e_{11}, and the permittivity ϵ_1 of 4.9×10^{-4}, 1.6×10^{-3}, and 2.8×10^{-4}, respectively.[30] These changes are negligible in the present experiments; hence, temperature effects will be neglected.

B. Electrostatic Configuration

The propagation of an elastic shock wave through a piezoelectric solid with short-circuited electrodes will be described in terms of the electrostatic configuration shown in Fig. 3. A section through a one-dimensional region of the disk shows the shock front at a typical time before traversing the thickness of the disk. In moving from left to right, the shock front divides the disk into two characteristic electrostatic regions. In the region behind the shock front the sample is strained to a constant value of piezoelectric polarization P_η. To accommodate the short-circuited condition between the electrodes, time-dependent electric fields $E(t)$ are developed with polarities as shown. The left face of the disk moves with particle velocity u. The polarization, strain, and electric fields are collinear along the x axis of the disk.

The shock wave moves with a speed slow compared to the speed of an electromagnetic disturbance; hence, the analysis utilizes electrostatic solutions and neglects electromechanical coupling effects. Since quartz has a small value for electromechanical coupling, the weak-coupling solution provides an excellent approximation to the present experiments and the electromechanical coupling effects can be treated as a small perturbation to the electrostatic solution.

C. Electrostatic Analysis

It is convenient to define the electric displacement D as

$$D = P_\eta + \epsilon E , \tag{15}$$

where P_η is the piezoelectric polarization and ϵ is the permittivity. The analysis will obtain a solution for the displacement current i,

$$i = A\frac{dD}{dt} , \tag{16}$$

where A is the area of the collecting electrode. If there is no free charge in the disk, i.e., the conductivity[31] equals zero, $\nabla\cdot\vec{D}=0$; hence, for the one-dimensional case,

$$\frac{\partial D}{\partial x} = 0 . \tag{17}$$

The electrical short circuit imposes the following condition between the electrodes:

$$\int_{\text{thickness}} E(x)\,dx = 0 . \tag{18}$$

The basic conditions expressed in Eqs. (15)–(18) can be readily applied to the particular configuration used in these experiments. The short-circuit condition of Eq. (18) leads to

$$E_1(t)l_1(t) + E_2(t)l_2(t) = 0 , \tag{19}$$

where l_1 and l_2 are the time-dependent thicknesses of the unstressed and stressed regions. From Eq. (17) it follows that

$$P_\eta + \epsilon_2 E_2 = \epsilon_1 E_1 . \tag{20}$$

Equations (19) and (20) thus lead to the result that

$$D = \epsilon_1 E_1 = P_\eta[1 + \alpha l_1(t)/l_2(t)]^{-1} , \tag{21}$$

where α is the ratio of the strained-to-unstrained permittivity ϵ_2/ϵ_1; $l_1 = l_0 - Ut$; and $l_2 = (U-u)t$. The displacement current is then

$$\frac{i(t)t_0}{P_\eta A} = \frac{\alpha(1-u/U)}{[(1-u/U)\,(t/t_0) + \alpha(1-t/t_0)]^2} , \quad 0 < t < t_0 \tag{22}$$

where $t_0 = l_0U^{-1}$, the shock-wave transit time.

In the normalized form shown in Eq. (22), the current is close to a unit step function. This is apparent when the maximum value of $u/U = 0.04$ and the maximum value of $\alpha = 1.02$ are substituted into the equation. The form of this solution is in

good agreement with the experimentally observed current pulses shown in Fig. 2. This good agreement serves to demonstrate the validity of the model.

It will be convenient to analyze the data with the value of current at $t=0$ called i_i, and the current at shock-wave transit time t_0, called i_f. From Eq. (22) we see that

$$i_f/i_i = \alpha^2(1-u/U)^{-2}. \tag{23}$$

Thus, this ratio of currents provides an experimental measure of the ratio of the strained-to-unstrained permittivity. The current value when the shock enters the disk provides a direct convenient measure of the piezoelectric polarization. From Eq. (22),

$$P_n = \frac{t_0\alpha}{A(1-u/U)}\, i_i. \tag{24}$$

The direct relation between current and piezoelectric polarization shown in Eq. (24) allows each current measurement at a particular strain to serve as a direct measure of the polarization. The electrostatic model leading to Eq. (24) does not include the effect of electromechanical coupling on the current wave shape; however, a small correction to the basic model will permit accurate solutions which incorporate electromechanical coupling.

D. Electromechanical Coupling

Several authors have obtained analytical solutions for the effect of electromechanical coupling on a short-circuited current from piezoelectric disks.[32-34] The total correction to the polarization computed from the electrostatic model is only about 1% for the present experiments; however, the accuracy of the present experiments makes this correction necessary. Stuetzer[32] has shown that electromechanical coupling has the effect of modifying the step-function current pulse in such a way that $i(t) = i_i\, e^{Bk^2t/t_0}$, where k^2 is the electromechanical coupling, $e_{11}^2/\epsilon_1^S c_{11}^D = 0.0084$,[21] and B is a constant which depends upon the acoustical boundary conditions at the electrodes. Values for B are 1.0, 1.5, or 2.0 depending upon whether the acoustic impedances of the two electrodes are, respectively, matched-matched, matched-free, or free-free.

For the present experiments the configuration is acoustically matched at the input electrode and has Epoxy potting with an acoustic impedance one-fifth the value of X-cut quartz on the opposite face. In addition to the Epoxy, a solder joint and wire connect to the electrode remote from the impact face. Linear interpolation with the acoustic impedance shows that the Epoxy would cause a value of $B=1.4$. Our low-strain experiment in which the current-time response is measured provides a direct measure of $i(t)$ which is in good agreement with $B=1.4$. These considerations lead to the result that the ratio of currents at small strains R caused by electromechanical coupling is $R = e^{1.4k^2}$. A small increase in R with strain is anticipated from the preliminary data analysis which determines values for e_{11}, ϵ_{11}, and c_{11} at large strains. From these results it follows that

$$R(\gamma) = 1.012 + 0.28\gamma. \tag{25}$$

The initial current-jump value i_i used to compute the piezoelectric polarization is unaffected by electromechanical coupling. However, the experimentally observed ratio of final current to initial current, i_f/i_i, includes a contribution due to the electromechanical coupling. Thus, the value of α corresponding to the ratio of the permittivity of the strained-to-unstrained material is less than that predicted in the electrostatic model without electromechanical coupling. The computation of a value for α which includes correction for electromechanical coupling is then

$$\alpha = (1-u/U)[1+(i_f/i_i)-R]^{1/2}. \tag{26}$$

The electrostatic analysis with minor modification for electromechanical coupling is used to analyze each current-pulse measurement. The piezoelectric pulse analysis indicates that piezoelectric polarization may be computed from the value of the current jump i_i with the aid of Eq. (24). The value of α used in Eq. (24) is obtained from a best fit to the values of α computed from Eq. (26).

V. RESULTS

Experiments were conducted over a large range of strain (2.4×10^{-3}–7×10^{-2}) to determine the limit of elastic response. Experiments at strains from 4.3×10^{-2} to 7×10^{-2} were observed to show current-time wave shapes with highly nonlinear behavior which became increasingly pronounced with increasing strain. The distorted wave shapes indicate that the model proposed in Sec. IV is insufficient to determine the piezoelectric response for strains greater than 4.3×10^{-2}. The current pulses are consistent with that expected from inelastic response[35] and serve to show that the limit of elastic response in shock-loaded X-cut quartz is 4.3×10^{-2}. Accordingly, the results to be shown are limited to the experiments at strains less than this elastic limit.

To determine the piezoelectric polarization from the observed current pulses, the shock velocity vs input particle velocity and the current-ratio data were represented by statistical fits. To improve the statistical confidence in the result, wave-velocity data from the previous study[11] for strains between 2.5×10^{-2} and 4.3×10^{-2} are included with measurements from the present investigation. A linear fit to the data gives the result

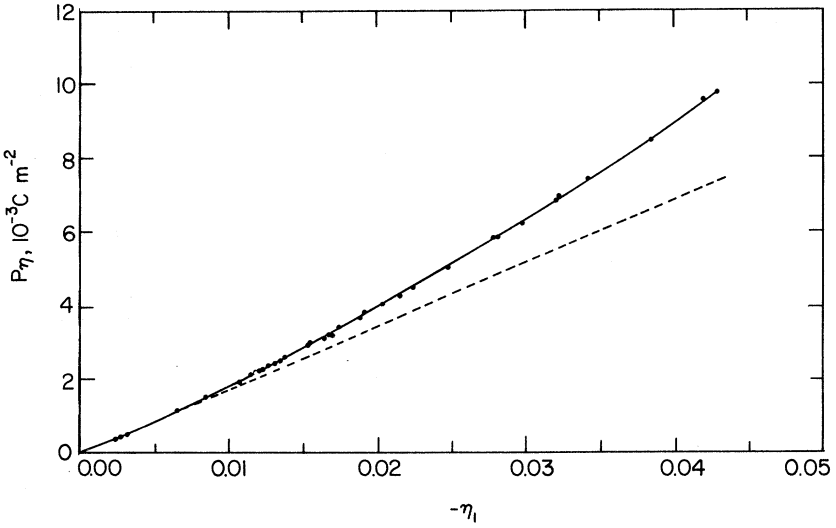

FIG. 4. Piezoelectric polarization P_η observed at various compressive strains. The dashed line is plotted to illustrate the linear response which would be observed if the direct nonlinear constant were zero. The line through the data is a plot of the quadratic fit which is observed to give an excellent representation to the data. The difference between the observed polarization and the dashed line serves to illustrate the contribution of the nonlinear constant at the various strains.

$$U(u) = [(5.724 \pm 0.018) + (0.312 \pm 0.112)u] \times 10^3 \text{ m sec}^{-1}, \quad (27)$$

where the ± indicates the standard error and $u_{max} = 250$ m sec^{-1}. The experimental error of ± 0.5% is felt to be the major contributor to the standard error.

Even though the wave-velocity measurements are not as precise as would be desirable, it should be observed that the piezoelectric-constant values determined in the present configuration are independent of the wave velocity. This result is readily obtained by observing that the polarization, Eq. (24), and strain, Eq. (13), are both inversely proportional to the velocity; hence, the ratio of polarization to strain is independent of wave velocity.

The experimentally observed ratios of final current to initial current are represented by a linear least-squares fit which expresses the value for the strain dependence of α as

$$\alpha = 0.9996 + (0.463 \pm 0.130)\gamma. \quad (28)$$

Unfortunately, for strains greater than 3×10^{-2} the current-vs-time pulses showed evidence of shock-induced conductivity. The conductivity was relatively small and did not affect the first current values i_i from which the polarization was computed. However, final current values i_f were sufficiently changed by the conductivity such that values of α could not be calculated from the experimental data in this strain range. The value of α is not likely to undergo an abrupt change; hence, the values for α determined up to 3×10^{-2} are linearly extrapolated to strains up to 4.3×10^{-2} to interpret the large-strain data.

Piezoelectric-polarization values were calculated with the aid of Eqs. (24), (27), and (28) for each of 35 measured current pulses. The resulting piezoelectric-polarization values are plotted against the quadratic strain in Fig. 4.

To aid in interpretation of the nonlinear effects, a line with slope equal to the linear constant is shown. The difference between the linear contribution and the observed polarization is that due to the nonlinear contribution. It can be readily observed that the experiments utilize strain for which the nonlinear contribution is negligible as well as strains for which the nonlinear contribution is pronounced.

The line drawn through the data is a quadratic least-squares fit. It is apparent that the quadratic fit gives an excellent representation to the data. This observation confirms that the form of the piezoelectric constitutive relation expressed in Eq. (10) provides an excellent quantitative representation to the response of X-cut quartz to strains as large as 4.3×10^{-2}. The data further demonstrate that contributions of higher-order terms are negligibly small ($\partial^2 e_{11}/\partial\eta_1^2 < \sim 10^{-1}$ C m^{-2}).

The quadratic fit to the piezoelectric-polarization data yields the result

$$P_\eta = (0.1711 \pm 0.00094)\eta_1 + (1.32 \pm 0.024)\eta_1^2, \quad (29)$$

where the units are C m^{-2}. The linear term is the value of the e_{11} piezoelectric stress constant, and the second term is a value for $\frac{1}{2}(\partial e_{11}/\partial\eta_1)$. The measurements provide a value for the linear constant with a standard error of 0.55%, the most accurate value achieved to date for this constant. The nonlinear constant is obtained with a standard error of 1.9%. Since the standard errors are consistent with the experimental errors, the material exhibited sample-to-sample variations which were significantly less than the experimental error.

A quadratic fit to the data for strains less than 3×10^{-2}, where conductivity was not observed,

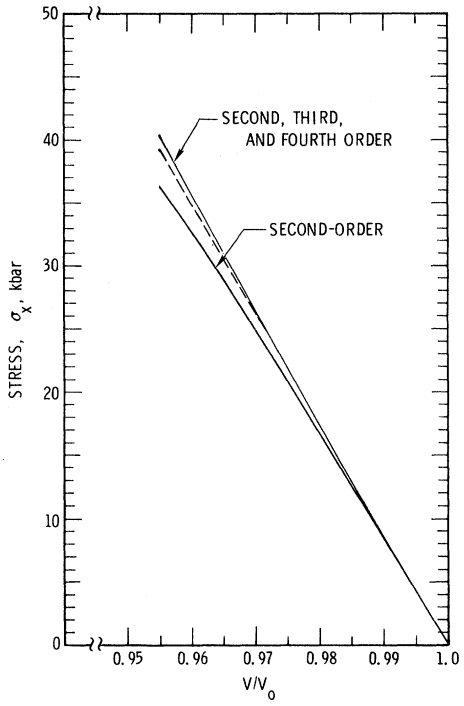

FIG. 5. Stress–vs–relative-volume relation which describes the elastic compression of X-cut quartz. The observed data are best fit by the line which includes second-, third-, and fourth-order constants. To illustrate the contributions of the various constants, the calculated stress-volume relation for the second-order constant alone is shown along with that of the second- plus third-order constant (dashed line).

shows the same coefficients as those obtained over the entire strain range. This observation indicates that the conductivity at the higher strains did not mask any unusual change in the piezoelectric response.

Determination of high-order elastic constants from elastic-shock-compression data is fully described in a recent paper[8] describing similar measurements for sapphire and fused quartz. The present paper follows the methods previously developed to accomplish a fit to the stress-vs-compression data which is obtained from the shock-velocity–particle-velocity measurements. In the data analysis, each shock-velocity–particle-velocity pair is used to compute a stress linear compression point from the conservation of momentum and mass, Eqs. (11) and (12). These data are then fit to a finite-strain constitutive relation by a method of successive approximations. At any particular strain the thermodynamic tension includes contributions from all the coefficients; however, the individual contributions can be separated provided experiments are accomplished over a wide range of strain. In the present case, the various t_1 values range from those for which the second-order constant represents the only detectable contribution, to those in which both the second- and third-order constants represent the only detectable contribution, to those in which second-, third-, and fourth-order constants all cause significant contributions. Thus, even though a single experiment cannot provide unique values for all coefficients, the complete set of experiments provides unique values for all coefficients since the experiments include the entire range of compression for which the various contributions are experimentally significant.

The present experiments lead to the stress–vs–relative-volume relations shown in Fig. 5. The contribution of the various constants is illustrated by separating the response into the contributions from the second-order coefficient alone, the second- plus third-order coefficient, and the observed stress–vs–relative-volume relation which is fit by the second-, third-, and fourth-order coefficients. The finite-strain elastic constants which fit the data are

$$c_{11} = (+0.868 \pm 0.0095) \times 10^{12} \text{ dyn/cm}^2,$$

$$c_{111} = (-3.0 \pm 0.3) \times 10^{12} \text{ dyn/cm}^2,$$

$$c_{1111} = (+75 \pm 25) \times 10^{12} \text{ dyn/cm}^2.$$

VI. DISCUSSION

Nonlinear acoustics and nonlinear interactions among acoustic,[3] optical,[36] and electrical fields[4] are ordinarily concerned with expressions for nonlinear properties evaluated as derivatives taken near the unstrained position. In that situation the nonlinear constants can be related to the fundamental lattice dynamical anharmonic effects. Typical experiments to evaluate high-order elastic constants, for example, are accomplished at strains less than about 10^{-4}. Since the maximum strains in the ultrasonic experiments are small, the nonlinear properties are expected to be representative of states at the unstrained condition.

The very large elastic limit which X-cut quartz exhibits under shock-wave compression allows the present measurements to be accomplished at large ($>10^{-4}$) strains. Nonlinear contributions which are small and difficult to detect under acoustic conditions are substantial and relatively easy to measure under elastic shock-compression conditions. The smallest strains of the present work are larger than those ordinarily employed in acoustic measurements; as such, the present measurements extend acoustic measurements of nonlinear properties by several orders of magnitude in strain. Even though the present measurements represent the response of the solid at the large strains employed in the investigations, it is only through comparison to linear and nonlinear acoustic values that smooth

TABLE I. Piezoelectric stress constant e_{11} (C m^{-2}). (± indicates standard error).

Bechmann (1958)[a]	0.171
Koga *et al.* (1958)[b]	0.174
Graham *et al.* (1965)[c]	0.174 ± 0.003
Present work	0.1711 ± 0.000 94

[a]Reference 21. [b]Reference 37. [c]Reference 11.

extrapolation to the unstrained state can be finally assured.

While the maximum strain employed in the present investigation is substantial (4.3×10^{-2}), it is not massive; hence, one would hope that in many cases the conditions are characteristic of continuous changes from the unstrained position. In fact, any observed deviation from a continuous change is cause for considerable concern since the discontinuous behavior could possibly be a result of inelastic effects.

Some evidence for a discontinuous change in piezoelectric polarization with strain was observed in the previous investigation of the piezoelectric properties of shock-loaded X-cut quartz.[11] Contrary to the previous observations, the present investigation, conducted with improved accuracy and better controlled experimental conditions, shows a continuous increase of polarization with strain.

A. Piezoelectric Constitutive Relation

1. Linear Piezoelectric Stress Constant

The continuously increasing piezoelectric polarization shown in the present investigation indicates a smooth extrapolation to zero strain. Inspection of Fig. 4 demonstrates that the nonlinear piezoelectric polarization produces a negligible contribution at the lowest strains; as the strains increase, the nonlinear contribution increases smoothly from the low-strain values. The smoothly increasing polarization combined with the excellent precision of the measurements are strong evidence that the linear constant obtained is representative of conditions at the unstrained state.

The linear piezoelectric stress constant e_{11} obtained in the present investigation is compared to values obtained by previous investigators in Table I. The present work provides the most accurate value achieved to date. The measurements provide values with a standard error of 0.55%. The maximum experimental error does not exceed ±1%.

Previous authors have utilized the elastic-shock-compression technique to determine the piezoelectric current response of X-cut quartz at reduced[38] and elevated temperatures.[39] Even though these measurements are not as complete as those reported in the present investigation and smooth extrapolation to the unstrained state is somewhat uncertain, the data of the present paper give some confidence in the extrapolation. The values obtained by analyzing the data with the present model are shown in Table II.

Over the temperature interval 295–573 °K, a temperature coefficient of $\Delta e_{11}/e_{11}\Delta T = -1.5\times10^{-4}\,^{\circ}\mathrm{C}^{-1}$ is obtained. This value should be compared to the small-signal measurement[30] of $-1.6\times10^{-4}\,^{\circ}\mathrm{C}^{-1}$ from 288 to 319 °K. Between 295 and 790 °K the elastic-shock-compression measurements show a value of $\Delta e_{11}/e_{11}\Delta T = -1.6\times10^{-4}\,^{\circ}\mathrm{C}^{-1}$.

2. Nonlinear Piezoelectric Stress Constant

The nonlinear piezoelectric stress constant for the direct piezoelectric effect, $\partial e_{11}/\partial\eta_1$, is the most unique measurement reported in the present paper. The present measurements provide the first quantitative value for the strain dependence of a piezoelectric constant in any solid. Nonlinear piezoelectric constants are of particular interest at present because of microwave acoustical studies of piezoelectric solids.[4,40] Furthermore, acoustic second-harmonic generation at microwave frequencies[41] and surface-wave microwave responses[41,42] may be utilized to detect nonlinear piezoelectric response. Recently, microwave surface-wave experiments have been employed to determine values for the combined nonlinear elastic, piezoelectric, and dielectric surface-wave contributions in several materials.[43]

Based on the present model the data from the previous elastic compression study at room temperature[11] can be analyzed to yield a value for the nonlinear constant. The value obtained is $\partial e_{11}/\partial\eta = -2.94\pm0.25$ C m^{-2}. Although the standard error is appreciable, 8.5%, the value is in reasonable agreement with the present value (-2.64 ± 0.048). The nonlinear constant can also be compared to that obtained from the acoustic second-harmonic-generation experiments of Carr and Slobodnik,[44] who estimated the constant to lie between -0.5 to -7 C m^{-2}. This order-of-magnitude estimate is in agreement with the present value.

The Maxwell relations for a piezoelectric solid[4,45] can be employed to demonstrate that $\partial e_{11}/\partial\eta_1 = -\partial c_{11}/\partial E_1$. Although the recent realization[17–19]

TABLE II. Piezoelectric stress constants at various temperatures (C m^{-2}). (± indicates standard error.)

Temperature (°K)	e_{11}	$\frac{\partial e_{11}}{\partial\eta_1}$	Reference
79	0.177 ± 0.003	−1.1 ± 0.15	a
295	0.1711 ± 0.000 94	−2.64 ± 0.048	Present work
573	0.164 ± 0.0024	−2.8 ± 0.24	b

[a]Computed from the data of Jones (Ref. 38).
[b]Calculated from the data of Rohde and Jones (Ref. 39).

that the conventional form of the internal-energy function utilized to obtain this identify is thermodynamically inconsistent, it is nevertheless interesting to compare the experimental values obtained in the two experiments. Hruska[46] has obtained a value of $\partial c_{11}/\partial E_1 = 2.6$ with a standard error of about 0.8. Although of limited accuracy, the value is in good agreement with the present value. It would be of considerable interest to accomplish more accurate measurements of the field dependence of the c_{11} constant for comparison with the present value.

Although measurement of piezoelectric constants under hydrostatic compression involves several nonlinear contributions, the results are of interest. Jones[47] measured the pressure dependence of the piezoelectric strain constant d_{11} to 3 kbar and showed that $d_{11}(P) = d_{11}(0)(1+\beta P)$, where P is the pressure in kbar and $\beta = (6.3 \pm 1.1) \times 10^{-3}$ kbar^{-1}. His results indicate a nonlinear dependence which is of the same order of magnitude as that observed for the strain dependence.

The temperature dependence of the nonlinear constant can be estimated from the previous elastic shock-compression measurements[38,39] at elevated and reduced temperatures. Although insufficient data are available to assign accurate values for α needed in the analysis, approximate values can be obtained for the piezoelectric polarization by letting $\alpha = 1.0$ at all strains. The values obtained from an analysis of the elevated and reduced temperature data based on the present model are shown in Table II. At 573 °K, in contrast to the behavior of the linear constant, the nonlinear constant is observed to be little changed from the room-temperature value. The standard error is large enough, however, to permit a significant temperature dependence to exist. At liquid-nitrogen temperature there is a significant decrease in the nonlinear constant even though the linear constant increases in value.

There is presently no basic theory to relate the direct effect nonlinear piezoelectric constant to fundamental properties of the solid. Several authors[4,20] have suggested that Miller's rule[48] relating nonlinear optical properties to susceptibility could be extended to nonlinear piezoelectric constants. However, Miller's rule has been shown to be a specific case of a more general theory based on the ionicity of the crystal lattice.[49] When additional quantitative measurements of nonlinear piezoelectric constants are obtained on other solids, it may be of interest to apply similar theoretical techniques to the study of nonlinear piezoelectric effects.

3. *Strain Dependence of Permittivity*

The electrostatic analysis developed in Sec. IV demonstrates that the ratio of the strained to unstrained permittivity, α, is directly related to the ratio of initial current jump when the shock front first enters the sample to the current when the shock reaches the rear electrode. This electrostatic model, with a correction applied for electromechanical coupling, was utilized to determine values for the strain dependence of α from the experimentally observed current pulses at various strains. Since $\epsilon_{11}^{-1}(\partial\epsilon_{11}/\partial\eta_1) = 1 - \alpha$ and $\alpha \approx 1$, the value obtained for the strain dependence of the permittivity is inaccurate but quantitative. The least-squares fit to the data represented by Eq. (28) gives a value of

$$\epsilon_{11}^{-1}\frac{\partial\epsilon_{11}}{\partial\eta_1} = -0.46 \pm 0.13\,,$$

where the ± indicates the standard error.

Lysne[50] has performed elastic shock-compression experiments with thin X-cut quartz disks subjected to multiply reverberating waves. He utilized a different form for the constitutive relations in order to develop expressions for electromechanical current distortions for many wave reverberations. His data can be analyzed to yield a value $\epsilon_{11}^{-1}(\partial\epsilon_{11}/\partial\eta_1) = -0.5$. This is in good agreement with the present value.

Since the strain dependence of permittivity has not been measured previously, several authors[4,20,44] have applied thermodynamic identities to estimate values for this constant from the photoelastic constant. There appears to be little physical basis for such a calculation since the elasto-optic constants are measured at optical frequencies which yield only the electronic contribution to permittivity. Ultrasonic frequency values, on the other hand, include contributions from electronic and lattice polarizability. Nevertheless, it is of interest to note that the value of the strain dependence of the permittivity deduced from the photoelastic constant is in reasonable agreement with our measurements.

Carr and Slobodnik[44] have related the constants directly through the relation

$$\epsilon_{11}^{-1}\frac{\partial\epsilon_{11}}{\partial\eta_1} = -\frac{\epsilon_1}{\epsilon_0}\,p_{11} \tag{30}$$

which neglects the frequency difference of the two experiments. McMahon[20] relates the two constants by applying a frequency correction proportional to the square of the ratio of the susceptibilities. When this frequency correction is employed,

$$\epsilon_{11}^{-1}\left(\frac{\partial\epsilon_{11}}{\partial\eta_1}\right) = -\frac{\epsilon_0}{\epsilon_{11}}\,\chi^2\left(\frac{n^2}{n^2-1}\right)^2 p_{11}\,, \tag{31}$$

where χ is the ultrasonic frequency susceptibility and n is the refractive index. With a value of $p_{11} = 0.138$ (Ref. 30) and $n = 1.5$ (Ref. 51), the strain dependence of the permittivity is calculated to be -0.62 and -1.12 for the directly related and fre-

TABLE III. Elastic constants of X-cut quartz (10^{12} dyn cm^{-2}).

	c_{11}	c_{111}	c_{1111}
McSkimin[a]	0.8680	•••	•••
Thurston[b]	•••	−2.1	•••
Fowles[c]	•••	•••	+160
Present work[d]	0.868 ± 0.0095	−3.0 ± 0.3	+75 ± 25

[a]Reference 57.
[b]Reference 22.
[c]Reference 15.
[d]± indicates a maximum error based on experimental precision.

quency-corrected calculations, respectively. Thus, it appears that a reasonable estimate for the strain dependence of the permittivity of X-cut quartz can be calculated from the elasto-optic constant if no frequency correction is applied.

A somewhat similar situation obtains for sapphire (α-Al_2O_3). Previously reported measurements[52] of the change in permittivity of sapphire subjected to elastic shock compression along the z axis can be analyzed to show that

$$\epsilon_{33}^{-1}\frac{\partial\epsilon_{33}}{\partial\eta_3} = +2.39 \pm 0.044 .$$

This value can be compared to the elasto-optic data with $n = 1.768$ (Ref. 53), $p_3 = -0.30$ (Ref. 53), and $\epsilon_{33}/\epsilon_0 = 11.55$ (Ref. 54). Equation (30), which utilizes no frequency correction, predicts a value $\epsilon_{33}^{-1}(\partial\epsilon_{33}/\partial\eta_1) = +3.4$, while Eq. (31), which applies a frequency correction, predicts a value of +4.2. Thus it appears that a reasonable estimate of the strain dependence of the permittivity of both X-cut quartz and Z-cut sapphire can be obtained from elasto-optic data on the basis of Eq. (30). This agreement is believed to be somewhat fortuitous and is probably related to the fact that the static and high-frequency dielectric constants for quartz and sapphire are not vastly different. Particularly in view of the increased interest in photoelastic constants,[55] the relationship between elasto-optic constants and the strain dependence of permittivity appears to warrant further investigation.

B. Elastic Constitutive Relation

The elastic constants obtained from the present investigation are compared to values reported by other investigators in Table III. Good agreement for the high-order constants is not achieved between the various investigators.

The fourth-order constant reported by Fowles[15] was obtained from measurements over a limited range of strain. Furthermore, his value was obtained by assuming that the ultrasonic third-order constant was representative of the large-strain response and the question of extrapolating the ultrasonic values to large elastic strains was not critically examined. The experiments also involved inelastic response. For these reasons, the present value is better established and is to be preferred.

The difference between the third-order constant obtained ultrasonically and under elastic shock compression is larger than can be accounted for from the various experimental errors. The two values lead to quite different descriptions for the propagation of a finite-amplitude strain wave. Thurston[56] has pointed out that a linear elastic response is obtained if $c_{111} = -3c_{11}$ and that dispersion in the wave profile will be obtained if $c_{111} < -3c_{11}$. On the basis of the ultrasonic value[57] of $c_{111} = -2.6c_{11}$, a step-function strain wave of 10^{-2} would be expected to disperse to a ramp wave whose rise is about 2 nsec/mm of travel.

The present experiments show that $c_{111} = -3.46c_{11}$ and show no evidence for dispersive behavior even though both the wave transit time and current amplitude measurements are sensitive to wave speed and both are determined with different sample thicknesses. An unrealistically large value for the fourth-order constant would have to be invoked to maintain the steady-wave profile. This large value for the fourth-order constant would cause unrealistic response at the larger strains employed in the elastic shock-compression investigation. Thus there seems to be no way to bring the ultrasonic and elastic shock-compression values into agreement.

It should be noted, however, that Thurston *et al.* used various data-reduction weighting schemes to combine their uniaxial-stress and hydrostatic-pressure measurements. The best fit to their uniaxial-stress data alone shows $c_{111} = -2.6 \times 10^{12}$ dyn cm^{-2} with a standard error of 0.46. This value is in much better agreement with the present value. Thurston *et al.* also observed similar differences between their uniaxial-stress data and the combined data for the c_{333} constant.

It should be recalled that the elastic constitutive relation was developed with the "weak-coupling" approximation which neglects the piezoelectric contribution to stiffness. Since the nonlinear piezoelectric constants are now known, the piezoelectric stiffening terms for third- and fourth-order can be evaluated. The high-order piezoelectric coupling relations can be readily developed from Eq. (7) by noting that the electric field under open circuit (D = const) conditions is

$$\left(e_{11} + \frac{1}{2}\frac{\partial e_{11}}{\partial\eta_1}\eta_1\right)\eta_1\left(e_{11} + \frac{\partial\epsilon_{11}}{\partial\eta_1}\eta\right)^{-1} .$$

When this value of electric field is substituted into Eq. (7) and the thermodynamic identity $\partial e/\partial E = \partial\epsilon/\partial\eta$ is utilized, it follows that the open-circuit constants c_{11}^D, c_{111}^D, and c_{1111}^D can be expressed in terms of the internally short-circuited constants c_{11}^E, c_{111}^E, and c_{1111}^E as

$$c_{11}^D = c_{11}^E\left(1+\frac{e_{11}^2}{\epsilon_{11}c_{11}^E}\right),$$

$$c_{111}^D = c_{111}^E\left[1+\frac{3e_{11}}{\epsilon_{11}c_{111}^E}\left(\frac{\partial e_{11}}{\partial\eta_1}\right)-\frac{e_{11}^2}{\epsilon_{11}c_{111}^E}\left(\frac{1}{\epsilon_{11}}\frac{\partial\epsilon_{11}}{\partial\eta_1}\right)\right],$$

and

$$c_{1111}^D = c_{1111}^E\left[1+\frac{1}{\epsilon_{11}c_{1111}^E}\left(\frac{\partial e_{11}}{\partial\eta_1}\right)^2-\frac{3e_{11}}{\epsilon_{11}c_{1111}^E}\left(\frac{1}{\epsilon_{11}}\frac{\partial\epsilon_{11}}{\partial\eta_1}\right)\left(\frac{\partial e_{11}}{\partial\eta_1}\right)+\frac{e_{11}^2}{\epsilon_{11}c_{1111}^E}\left(\frac{1}{\epsilon_{11}}\frac{\partial\epsilon_{11}}{\partial\eta_1}\right)^2\right].$$

Substituting values from the present paper into these expressions gives the result that

$$c_{11}^D = c_{11}^E(1+0.0084),$$

$$c_{111}^D = c_{111}^E(1+0.11-0.0011),$$

and

$$c_{1111}^D = c_{1111}^E(1+0.023-0.0021+0.00002).$$

The contribution of piezoelectric stiffening to the third-order constants is calculated to be 11%. This value is large enough such that it should be observable in ultrasonic experiments conducted on low resistivity and open-circuited samples. The contributions to stiffening due to the nonlinear converse-effect constant $[(1/\epsilon)(\partial\epsilon/\partial\eta)]$ are noted to be very much less than the contribution of the direct-effect nonlinear constant $\partial e/\partial\eta$.

VII. SUMMARY

The present paper reports the first quantitative experimental measurement of a nonlinear piezoelectric constitutive relation. The measurements yield the most accurate value reported to date for the linear piezoelectric stress constant of X-cut quartz, the first quantitative measurement of a nonlinear piezoelectric constant for the direct effect, and a value for the strain dependence of the permittivity. The longitudinal finite-strain elastic constitutive relation for x-axis compression was determined with second-, third-, and fourth-order elastic-constant measurements which represent the compression of the solid to compressive strains up to 4.3×10^{-2}. The third-order constant value appears to differ significantly from the value determined from ultrasonic experiments. The technique seems generally applicable to the study of other piezoelectric solids which exhibit large elastic limits under shock-wave loading and should permit nonlinear piezoelectric constants to be studied in some detail.

ACKNOWLEDGMENTS

The author is pleased to acknowledge the unusually competent technical assistance of G. E. Ingram and R. D. Jacobson in carrying out the experimental measurements. Discussions with C. F. Quate, R. B. Thompson, and J. C. Crawford were extremely helpful in relating the present work to microwave acoustics. R. W. Rohde was kind enough to let the author examine his original data. Discussions with P. C. Lysne are also gratefully acknowledged. E. P. Eernisse and P. C. Lysne provided very helpful reviews of the manuscript. Discussions with G. A. Samara provided better insight into the dielectric-constant results.

*Work supported by the U. S. Atomic Energy Commission.

[1]For definitions of crystallographic orientations and piezoelectric constants see Proc. IRE 37, 1378 (1949).

[2]The direct piezoelectric effect causes a piezoelectric polarization upon application of a stress or strain. The converse piezoelectric effect, ordinarily utilized for measurements of piezoelectric constants, causes a strain upon application of an electric field. See, e.g., W. G. Cady [*Piezoelectricity* (Dover, New York, 1964), Vol. I]. The present experiments provide a measure of the strain dependence of a piezoelectric stress constant. This nonlinear constant will be referred to as the direct nonlinear piezoelectric stress constant to distinguish it from the converse nonlinear piezoelectric constant which describes the change of piezoelectric constant with electric field.

[3]L. K. Zarembo and V. A. Krasil'nikov, Usp. Fiz. Nauk 102, 549 (1970) [Sov. Phys. Usp. 13, 778 (1971)].

[4]R. B. Thompson and C. F. Quate, J. Appl. Phys. 42, 907 (1971).

[5]P. H. Carr, Phys. Rev. 169, 718 (1968).

[6]P. H. Carr and A. J. Slobodnik, Jr., J. Appl. Phys. 38, 5153 (1967).

[7]J. Holder and A. V. Granato, in *Physical Acoustics*, edited by Warren P. Mason and R. N. Thurston (Academic, New York, 1971), Vol. 8.

[8]R. A. Graham, J. Acoust. Soc. Am. 51, 1576 (1972).

[9]R. A. Graham, J. Appl. Phys. 32, 555 (1961).

[10]F. W. Neilson, W. B. Benedick, W. P. Brooks, R. A. Graham, and G. W. Anderson, *Les Ondes de Detonation* (Centre National de la Recherche Scientifique, Paris, France, 1962); also available as Sandia Laboratories Report No. SCR-416, 1961 (unpublished).

[11]R. A. Graham, F. W. Neilson, and W. B. Benedick, J. Appl. Phys. 36, 1775 (1965).

[12]R. A. Graham and W. J. Halpin, J. Appl. Phys. 39, 5077 (1968).

[13]R. A. Graham and G. E. Ingram, J. Appl. Phys. 43,

826 (1972).
[14]J. Wackerle, J. Appl. Phys. 33, 922 (1962).
[15]R. Fowles, J. Geophys. Res. 72, 5729 (1967).
[16]R. N. Thurston, in *Physical Acoustics*, edited by Warren P. Mason (Academic, New York, 1964), Vol. IA.
[17]R. A. Toupin, J. Ratl. Mech. Anal. 5, 859 (1956).
[18]A. C. Eringen, Int. J. Eng. Sci. 1, 127 (1963).
[19]H. F. Tiersten, Int. J. Eng. Sci. 9, 587 (1971).
[20]D. H. McMahon, J. Acoust. Soc. Am. 44, 1007 (1968).
[21]R. Bechmann, Phys. Rev. 110, 1060 (1958).
[22]R. N. Thurston, H. J. McSkimin, and P. Andreatch, Jr., J. Appl. Phys. 37, 267 (1966).
[23]R. A. Graham, J. Basic Eng. 89, 911 (1967).
[24]C. H. Karnes, in *Mechanical Behavior of Materials Under Dynamic Loads*, edited by U. S. Lindholm (Springer-Verlag, New York, 1968).
[25]G. E. Ingram and R. A. Graham, in *Proceedings of the Fifth Symposium on Detonation*, edited by S. Jacobs, also available on request as Sandia Laboratories Report No. SC-R-72 2722, 1972 (unpublished).
[26]S. Thunborg, Jr., G. E. Ingram, and R. A. Graham, Rev. Sci. Instr. 35, 11 (1964).
[27]See, e.g., G. E. Duvall and G. R. Fowles, in *High Pressure Physics and Chemistry*, edited by R. S. Bradley (Academic, New York, 1963), Vol. II.
[28]M. H. Rice, R. G. McQueen, and J. M. Walsh, in *Solid State Physics*, edited by F. Seitz and D. Turnbull (Academic, New York, 1958), Vol. VI.
[29]W. Herrmann, in *Wave Propagation in Solids* (The American Society of Mechanical Engineers, New York, 1970).
[30]See, R. Bechmann and R. F. S. Hearman, *Landolt-Bornstein Numerical Data and Functional Relationships in Science and Technology, New Series. Group III: Crystal and Solid State Physics* (Springer-Verlag, New York, 1966), Vol. I.
[31]Shock-induced conductivity in *X*-cut quartz has been carefully studied. Descriptions of the previous work are found in Refs. 12 and 13. Except for specific situations mentioned in Sec. V, these studies have shown the conductivity to be zero.
[32]O. M. Stuetzer, J. Appl. Phys. 38, 3901 (1967).
[33]M. Redwood, J. Acoust. Soc. Am. 33, 527 (1961).
[34]H. S. Chakraborty, Czech. J. Phys. B 19, 963 (1967).
[35]R. A. Graham and G. E. Ingram, Bull. Am. Phys. Soc. 14, 1163 (1969).
[36]M. Lax and D. F. Nelson, Phys. Rev. B 4, 3694 (1971).
[37]I. Koga, M. Aruga, and Y. Yoshinaka, Phys. Rev. 109, 1467 (1958).
[38]O. E. Jones, Rev. Sci. Instr. 38, 253 (1967).
[39]R. W. Rohde and O. E. Jones, Rev. Sci. Instr. 39, 313 (1968).
[40]A. A. Chaban, Zh. Eksperim. i Teor. Fiz. pis'ma v Redaktsiyu 6, 967 (1966) [Sov. Phys. JETP Letters 6, 381 (1967)].
[41]P. Thery, E. Bridoux, and M. Moriamez, J. Phys. C Suppl. 31, C1-29 (1970).
[42]R. M. White, Proc. IEEE 58, 1238 (1970).
[43]T. C. Lim, E. A. Kraut, and R. B. Thompson, Appl. Phys. Letters 20, 127 (1972).
[44]P. H. Carr and A. J. Slobodnik, Jr., J. Appl. Phys. 38, 5153 (1967).
[45]W. P. Mason, *Piezoelectric Crystals and their Applications to Ultrasonics* (Van Nostrand, Princeton, N. J., 1950), Appendix A-6.
[46]K. Hruska, IEEE Trans. Sonics Ultrasonics SU-18, 1 (1971). It should be noted that Hruska accomplished the first experimental measurement which involved a nonlinear piezoelectric effect. See K. Hruska, Czech. J. Phys. B 11, 150 (1961).
[47]M. R. Jones, Ph.D. dissertation (University of Utah, 1970) (unpublished).
[48]R. C. Miller, Appl. Phys. Letters 5, 17 (1964).
[49]B. F. Levine, Phys. Rev. Letters 22, 787 (1969).
[50]P. C. Lysne, J. Appl. Phys. 43, 425 (1972).
[51]*Handbook of Chemistry and Physics*, edited by C. D. Hodgman (The Chemical Rubber Publishing Co., Cleveland, Ohio, 1962).
[52]R. A. Graham and G. E. Ingram, in *Behavior of Dense Media Under High Dynamic Pressures* (Gordon and Breach, New York, 1968).
[53]T. A. Davis and K. Vedam, J. Appl. Phys. 38, 4555 (1967).
[54]R. D. Olt, Electronics 32, 110 (1959).
[55]D. F. Nelson and M. Lax, Phys. Rev. B 3, 2778 (1971).
[56]R. N. Thurston, J. Acoust. Soc. Am. 45, 1329 (1969).
[57]H. J. McSkimin, P. Andreatch, Jr., and R. W. Thurston, J. Appl. Phys. 36, 1624 (1965).

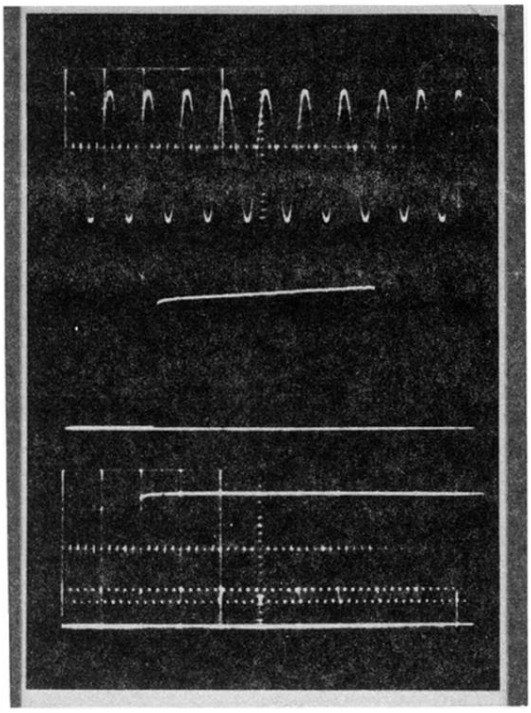

FIG. 2. Current amplitude vs time for a typical oscilloscope record is shown in the center trace. Time increases from left to right. The upper and lower traces are amplitude and timing calibration records taken immediately following the experiment. About 450 nsec prior to impact, the trace is triggered. The impact is indicated by the sharp jump in current followed by a gradual increase in current to shock-wave transit time which is indicated by a sharp decrease in signal amplitude 1.11 μsec after impact. The current amplitude is 0.67 A at a strain of 2.8×10^{-2}.